

A Coupled Cavity Microfluidic Dye Ring Laser

M. Gersborg-Hansen, S. Balslev, N. A. Mortensen, and A. Kristensen

Microfluidics Department of Micro and Nanotechnology,
Technical University of Denmark,
Building 345 East, Ørstedsparken, DK-2800 Kongens Lyngby, Denmark

Abstract

We present a laterally emitting, coupled cavity microfluidic dye ring laser, suitable for integration into lab-on-a-chip microsystems. The microfluidic laser has been successfully designed, fabricated, characterized and modelled. The resonator is formed by a microfluidic channel bounded by two isosceles triangle mirrors. The microfluidic laser structure is defined using photolithography in 10 μm thick SU-8 polymer on a glass substrate. The microfluidic channel is sealed by a glass lid, using PMMA adhesive bonding. The laser is characterized using the laser dye Rhodamine 6G dissolved in ethanol or ethylene glycol as the active gain medium, which is pumped through the microfluidic channel and laser resonator. The dye laser is optically pumped normal to the chip plane at 532 nm by a pulsed, frequency doubled Nd:YAG laser and lasing is observed with a threshold pump pulse energy flux of around $55 \text{ J}/\text{m}^2$. The lasing is multimode, and the laser has switchable output coupling into an integrated polymer planar waveguide. Tuning of the lasing wavelength is feasible by changing the dye/solvent properties.

Key words: Microfluidic dye laser, Rhodamine 6G, SU-8, PMMA

1 Introduction

Integrable lab-on-a-chip light sources are essential for on-chip spectral analysis of chemical samples [1]. For these applications dye lasers are of particular interest due to the possibility of tuning the wavelength in the visible range. Microfluidic dye lasers have recently been demonstrated by glass [2] and polymer [3] microfabrication and tunability has also been reported [4]. Polymer-based laterally emitting single-mode dye-lasers were reported recently [5]. The latter implementation is advantageous due to the direct integrability with lab-on-a-chip systems without additional hybridization steps [6].

In this paper we present a new type of polymer-based laterally emitting micro-uidic dye laser utilizing coupled cavities. Lasing is achieved with a new cavity design (see Fig. 1) relying on total internal reflection at the interface between the polymer (SU-8 with refractive index $n_1 = 1.59$) and the surrounding air at an incidence angle of 45° . Bleaching of the dye is avoided by a regenerating flow through the micro-uidic channel. In this way, the dye may also be dynamically changed, enabling real-time tunability of the laser. Furthermore, the output coupling is switchable.

In the following sections we describe the resonator structure, the fabrication, and the optical characterization. We also address the cavity mode spacing by a simple model and finally conclusions are given.

2 The resonator structure

The laser resonator, see Fig. 1, resembles a classical Fabry-Pérot resonator. A $100\text{ }\mu\text{m}$ wide $10\text{ }\mu\text{m}$ deep micro-uidic channel is bounded by two isosceles triangle mirrors formed in SU-8, giving rise to the laterally emitting ring laser cavity. This optical resonator relies on total internal reflection at the vertical sidewalls (a), (b), and (c) of the triangles, see Fig. 1. The laser dye gain medium is located in the micro-uidic channel passing through the cavity.

Out-coupling of the laser light is achieved by a second micro-uidic channel filled with ethanol, thereby removing the total internal reflection at the side (d) in the cavity. The out-coupled light is collected through an integrated planar 'output waveguide' (also in Fig. 1). The output coupling is switchable by alternating the content of the second uidic channel between ethanol and air. A metal mask with a transparent window at the resonator serves to localize the optical pumping light to the resonator and diminish unwanted fluorescence.

3 Fabrication

The fabrication sequence is schematically shown in Fig. 2. The process consists of two parts: Step 1-3 is a lift-off process to deposit the metal mask, 50 nm Cr and 250 nm Au, on a glass substrate, and step 4-8 is the forming of the micro-structures in SU-8, drilling, and bonding a glass lid on top.

In step 4 the micro-uidic laser structure, the integrated waveguide, and the micro-uidic channels (shown in Fig. 1) are defined by UV lithography on the substrate in a $10\text{ }\mu\text{m}$ thick layer of SU-8 photo resist [7]. Subsequent to development (step 5), the substrate is placed on a 150°C hotplate for $2\text{--}60\text{ s}$

which has the effect of healing the cracks in the SU-8 (step 6). After drilling the holes for the fluid inlets and outlets (step 7) the micro-fluidic channels are sealed in step 8 by bonding a glass lid on top by means of a 5 μm thick PMMA film [8]. The bonding is carried out at a temperature of 120 $^{\circ}\text{C}$ with a bonding force of 2 kN on a 4 inch wafer pair with a duration of 10 minutes.

4 Optical characterization

The laser structure is characterized using the laser dye Rhodamine 6G dissolved in i) ethanol and ii) ethylene glycol as the active gain medium, which is infused at 50 $\mu\text{L}/\text{h}$ through the micro-fluidic channel and laser resonator. The dye laser is optically pumped normal to the chip plane through the window (see Fig. 1) at 532 nm by a pulsed, frequency doubled Nd:YAG laser. The repetition rate is 10 Hz and the pulses have a duration of 5 ns.

The upper panels in Figs. 3 and 4 show typical output spectra with the dye dissolved in ethanol and ethylene glycol, respectively. The concentration is in both cases 2×10^{-2} mol/L. By increasing the pump pulse energy we observe an increase in the output intensity. The lower panels show the output power (numerically integrated output intensity) versus the pump pulse energy and the observed change of slope in the curves around $55 \text{ J}/\text{mm}^2$ is a clear signature of the onset of lasing for both solvents.

As shown in Fig. 5, the change of solvent introduces an over-all shift of the output spectra of approximately 2 nm. The red shift of the spectra measured using the ethylene glycol solution may be explained by a lower cavity-loss or a higher dye quantum efficiency using this solvent [9]. Since the dye/solvent properties can be changed dynamically this enables real-time tuning of the central lasing wavelength [4].

The output coupling from the structure is switched on by filling the second fluid channel (see Fig. 1) with ethanol, and it is switched off again by blowing air into the second channel or providing an under-pressure with a syringe, thereby sucking air through the second channel.

5 The cavity modes

The cavity mode spectrum has been modelled by a scattering matrix approach and Fig. 6 illustrates the 'unfolded' structure. Formally, the scattering matrix of the 'unfolded' structure is calculated and periodic boundary conditions are applied. In other words the ring resonator is formed by 'joining' the two ends

of the unfolded structure. This allows for calculation of the spectral position of the cavity modes. For the experimentally relevant parameters a mode spacing of approximately 0.13 nm is found.

Comparing to the experimental output spectra in Figs. 3 and 4 we might speculate that the sub-nanometer modulation of the overall peak resembles the longitudinal mode spacing. However, since the spectrometer resolution is around 0.15 nm the mode-spacing is not resolved experimentally. Compared to the estimated mode-spacing the overall width of the output spectra suggests that the lasing is longitudinally multimode.

6 Conclusion

We have demonstrated a laterally emitting coupled cavity micro-fluidic dye ring laser. The laser is fabricated with polymer technology using a total-internal reflection based cavity formed by two triangle mirrors. The light-source is straight forward to integrate with polymer planar waveguides for use in lab-on-a-chip devices. The dependence of the lasing wavelength on the dye solution may enable tunability. Using a simple modelling approach we estimated the mode-spacing of the order 0.13 nm which however can not be fully verified experimentally due to limited spectrometer resolution. We have shown the possibility of switching the output coupling which can be highly useful also in other applications.

Acknowledgements

The first author gratefully acknowledges financial support by Otto Mönstedts Fond and Geheimstatminister Greve Joachim Godske Moltkes Legat from Bergen ved Gods.

References

- [1] E. Verpoorte, Chip vision-optics for microchips, *Lab. Chip* 3 (2003) 42N {52N .
- [2] Y. Cheng, K. Sugiyoka, K. Midorikawa, Micro fluidic laser embedded in glass by three-dimensional femtosecond laser microprocessing, *Opt. Lett.* 29 (2004) 2007 { 2009.
- [3] B. Helbo, A. Kristensen, A. Menon, A micro-cavity fluidic dye laser, *J. Micromech. Microeng.* 13 (2003) 307 {311.

- [4] B. Bilenberg, B. Helbo, J. P. Kutter, A. Kristensen, Tunable microfluidic dye laser, in: Proceedings of the 12th Int. Conf. on Solid-State Sensors, Actuators and Microsystems, Transducers '03, Boston, MA, USA, 2003, pp. 206{209.
- [5] S. Balslev, A. Kristensen, High order bragg grating microfluidic dye laser, in: Proceedings of Conference on Lasers and Electro-Optics (CLEO) 2004, Vol. 96 of OSA Trends in Optics and Photonics, Optical Society of America, San Francisco, CA, USA, 2004, p. CM S6.
- [6] S. Balslev, B. Bilenberg, O. Geschke, A. M. Jrgensen, A. Kristensen, J. P. Kutter, K. B. Mogensen, D. Snakenborg, Fully integrated optical system for lab-on-a-chip applications, in: Proceedings of the 17th IEEE Conference on Micro Electro Mechanical Systems, MEMS 2004, Maastricht, the Netherlands, 2004, pp. 89{92.
- [7] SU-8 formulation 10 from MicroChem. Corp., www.microchem.com.
- [8] B. Bilenberg, T. Nielsen, B. Clausen, A. Kristensen, Pmma to su-8 bonding for polymer based lab-on-a-chip systems with integrated optics, J. Microtech. Microeng. 14 (2004) 814{818.
- [9] O. G. Peterson, J. P. Webb, W. C. McCollin, J. H. Eberly, Organic dye laser threshold, J. Appl. Phys. 42 (1971) 1917{1928.

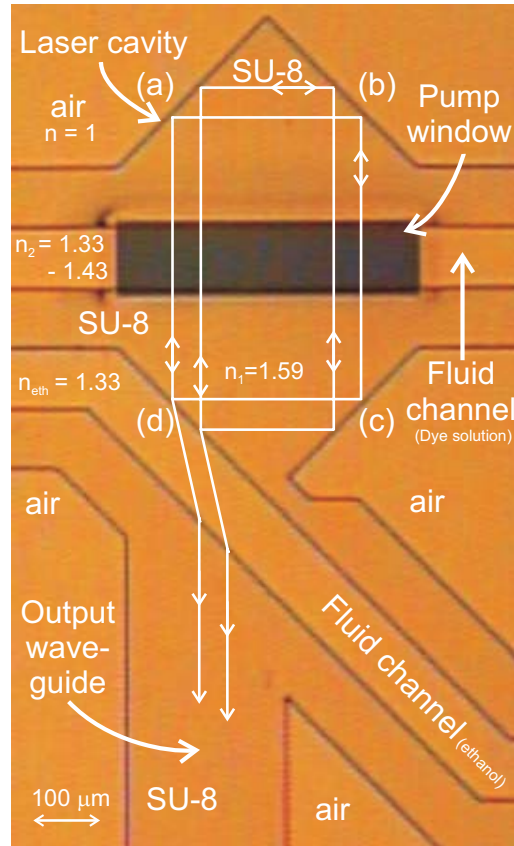


Fig. 1. Optical microscope image of the laser resonator structure consisting of two isosceles triangles of the photo de nable polymer SU-8 ($n_1 = 1.59$) and a microfluidic channel in-between. Two classical trajectories of equal optical path length are drawn. The optical pumping is performed through a window (dark rectangular area in the photo) in a metal mask.

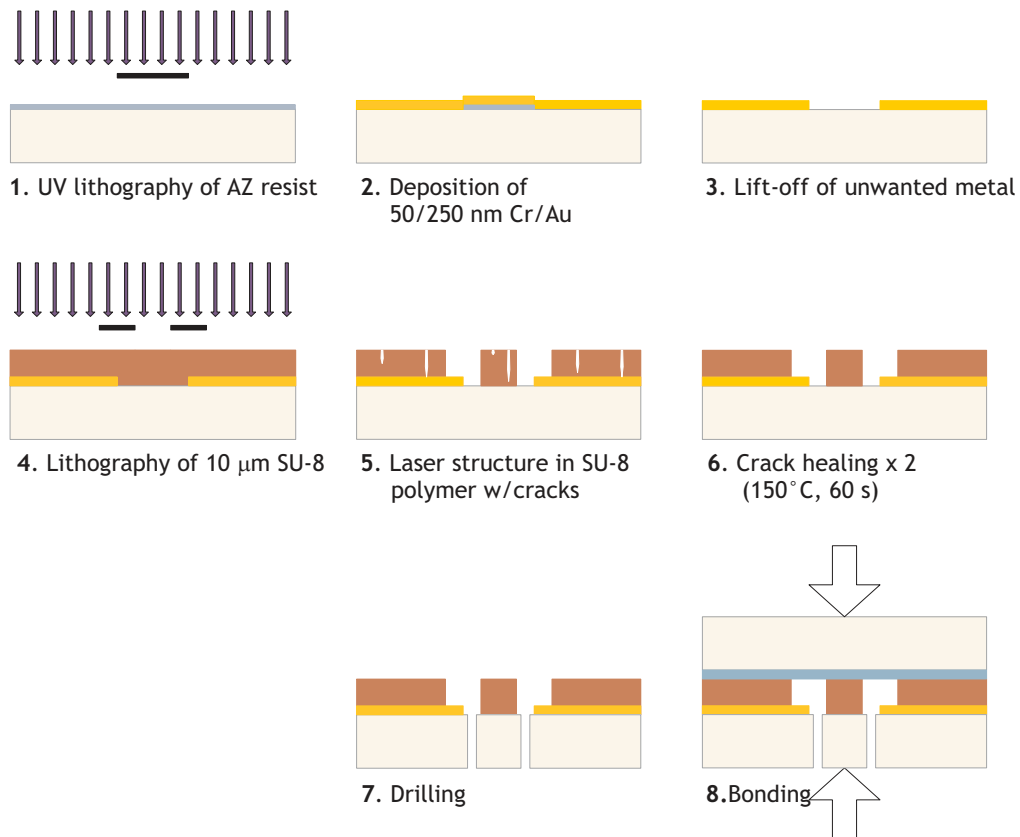


Fig. 2. A schematic of the fabrication sequence. Part 1-3: Lift-off process. The metal layer is used for screening the pumping light from certain areas of the chip to avoid unwanted fluorescence. Part 4-8: SU-8 lithography, drilling, and bonding.

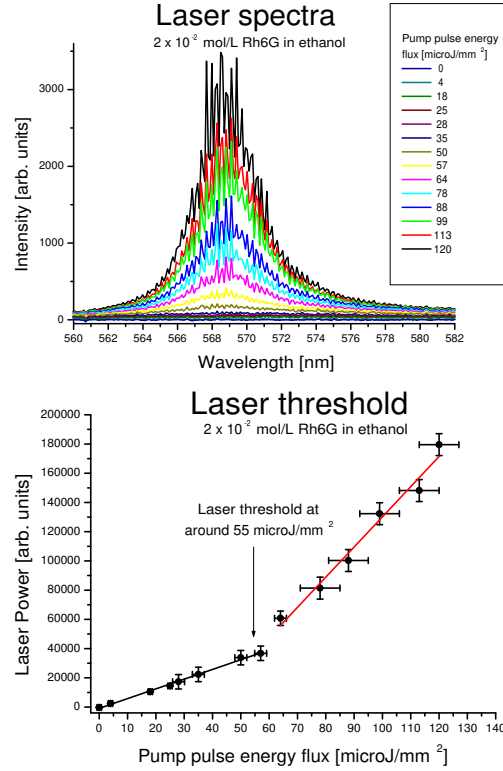


Fig. 3. Upper panel: Measured laser spectra using Rh6G dissolved in ethanol (2×10^{-2} mol/L) as the active gain medium at different pump pulse energy flux values. The dye laser is pumped at 532 nm using an external frequency doubled Nd:YAG laser. Lower panel: The laser power vs. the pump pulse energy flux for the spectra above. To obtain the laser power the optical output spectra have been numerically integrated from 550–600 nm. The linear dependence and change in slope reveals laser action. The lasing threshold is at about 55 $\text{J}/\text{m m}^2$.

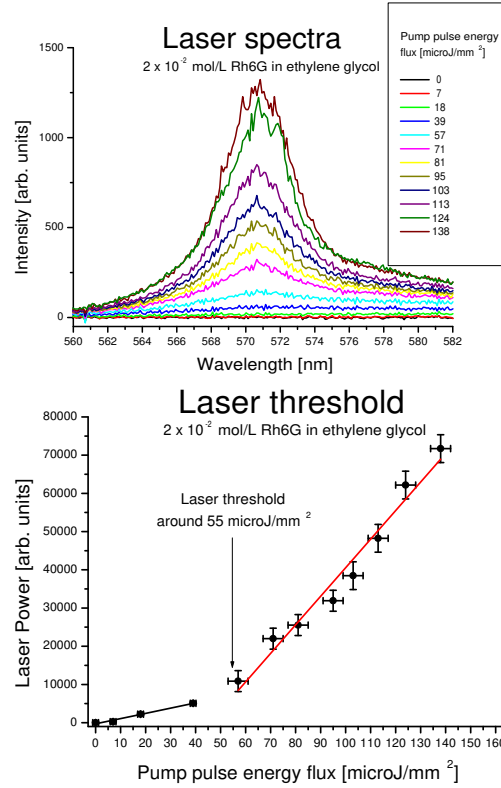


Fig. 4. Upper panel: Measured laser spectra using Rh6G dissolved in ethylene glycol (2×10^{-2} mol/L) as the active gain medium at different pump pulse energy flux values. The dye laser is pumped at 532 nm using an external frequency doubled Nd:YAG laser. Lower panel: The laser power vs. the pump pulse energy flux for the spectra above. To obtain the laser power the optical output spectra have been numerically integrated from 566–576 nm. The linear dependence and change in slope reveals laser action. The lasing threshold is at about 55 J/m^2 .

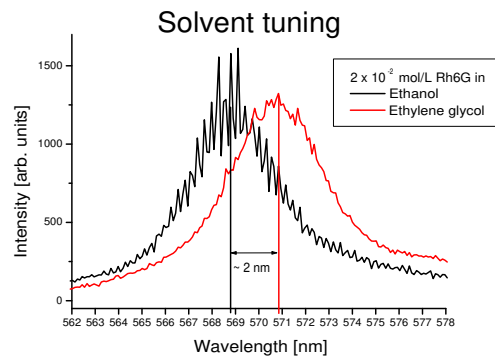


Fig. 5. Two measured laser spectra using Rh6G dissolved in ethanol and ethylene glycol, respectively, as the active gain medium (same concentration). The dye laser is pumped at 532 nm using an external frequency doubled Nd:YAG laser. The change of solvent provides tuning capabilities of the laser due to a shift of the gain spectrum of the dissolved laser dye. A red shift of approx. 2 nm is observed when changing from ethanol (refractive index $n = 1.33$) to ethylene glycol ($n = 1.43$).

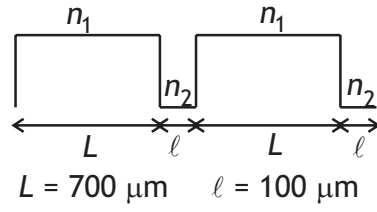


Fig. 6. For a calculation of the cavity mode spectrum the structure can effectively be 'unfolded'. The sketch illustrates the variation of the refractive index for one round-trip in the cavity depicted in Fig. 1. $n_1 = 1.59$, $n_2 = 1.33$ – 1.43 .